Original Russian Text © A. N. Morozov, E. V. Mankovskaya, 2022,
published in MORSKOY GIDROFIZICHESKIY ZHURNAL, Vol. 38, Iss. 5 (2022)

Characteristics of the Bottom Convective Layer of the Black Sea Based on *in-situ* Data (July, 2016)

A. N. Morozov ✉, E. V. Mankovskaya

Marine Hydrophysical Institute of RAS, Sevastopol, Russian Federation
✉ *anmorozov@mhi-ras.ru*

Abstract

Purpose. The purpose of the work is to detail the vertical structure of thermohaline characteristics near the upper boundary of the bottom convective layer based on the *CTD* measurements, to estimate the heat and salt fluxes, and to study variability of various layer characteristics depending on the geographic location of the stations.

Methods and Results. The data of the *SBE* 911*plus CTD* probe obtained in the 87th cruise of the R/V *Professor Vodyanitsky* which took place in June 30 – July 18, 2016 in the central sector of the northern Black Sea were used. The depth of the bottom convective layer upper boundary was revealed to be variable (1713–1922 m), on the average 1800 ± 60 m. Noted was a tendency for the upper boundary to rise by 150–200 m during transition from the western gyre to the eastern one. But at two stations, the layer was not observed up to the depths exceeding 1900 m. The variation range of potential temperature in the layer was $1.6 \cdot 10^{-3}$°C, and that of salinity – $1.2 \cdot 10^{-3}$ *psu*. Decrease both of the potential temperature and salinity in the bottom convective layer with increasing longitude and of potential temperature with the layer thickness increase was revealed. The coefficient of vertical turbulent diffusion at 150 m above the layer upper boundary was $1.1 \cdot 10^{-5}$ m^2/s. The calculated values of the heat and salt vertical fluxes in 150 m above the bottom convective layer upper boundary constituted 1.6 mW/m^2 and $2.9 \cdot 10^{-7}$ g/(m^2·s), respectively.

Conclusions. Having been analyzed, the data of contact deep-sea thermohaline measurements showed that the Black Sea bottom convective layer was unstable and spatially inhomogeneous, and the location of its upper boundary was variable. The data obtained permit to assume that the eddies penetrate to the deep layers of the sea and manifest themselves in significant deepening of the bottom convective layer upper boundary. In the western part of the sea, the bottom convective layer waters are warmer and saltier than those in its eastern part. Almost the entire geothermal heat flux is dissipated in the bottom layer. To maintain salt balance in the bottom convective layer, there should be a mechanism for replenishing salt in the lower layers of the sea.

Keywords: bottom convective layer, bottom layer, spatial variability, vertical mixing, vertical heat flux, vertical salt flux, Black Sea

Acknowledgments: the study was carried out within the framework of the state assignment on themes No. 0555-2021-0003 and No. 0555-2021-0005.

For citation: Morozov, A.N. and Mankovskaya, E.V., 2022. Characteristics of the Bottom Convective Layer of the Black Sea Based on *in-situ* Data (July, 2016). *Physical Oceanography*, 29(5), pp. 524-535. doi:10.22449/1573-160X-2022-5-524-535

DOI: 10.22449/1573-160X-2022-5-524-535

Introduction

Vertical thermohaline structure of the Black Sea waters has a number of features. One of them is the presence of a bottom homogeneous [1, 2] or convective [3–5] layer characterized by almost constant values of potential temperature and salinity throughout its entire thickness. Constancy in depth of hydrochemical [6] and hydrooptical [7] characteristics is also established in it. The layer is mainly formed due to convection supported by geothermal heat fluxes.

The bottom homogeneous layer existence in the Black Sea was first experimentally confirmed by the authors of [1] based on continuous CTD profiles obtained during five expeditions in 1988, which took place in the southern part of the sea. The upper boundary of the convective layer started from the horizon of 1700 m. The root-mean-square deviation from the mean value of potential temperature from region to region in the bottom convective layer (BCL) was $1.2 \cdot 10^{-3}$ °C, salinity – $2 \cdot 10^{-3}$‰. Later, focused deep-water measurements were carried out in 1997–2002 [4]. They confirmed the position of the BCL upper boundary and the variability ranges of its thermohaline characteristics in the eastern part of the sea. The study notes increased temperature and salinity gradients directly above the upper boundary of the layer. In recent works, based on field measurements, it has been shown that the bottom convective layer is not uniform and constant [5], and the deep-water Black Sea layers are more dynamically active [8] than previously thought. Focused measurements in the BCL in the northern Black Sea are not presented in the literature, which partly determines the relevance of the present study.

In recent years, Marine Hydrophysical Institute has been carrying out regular expeditions in the northern Black Sea, where hydrological measurements, including deep-sea ones, are traditionally taken [9]. During the summer expedition of 2016, 20 CTD profiles to depths exceeding 1900 m were obtained. The purpose of the work is to detail the vertical structure of thermohaline characteristics near the BCL upper boundary, to estimate the heat and salt fluxes, to study variability of various layer characteristics depending on the geographic location of the stations. The results of the work can be useful for clarifying the existing concepts of formation and evolution of the Black Sea bottom convective layer.

Materials and methods

The expedition materials obtained in the 87th cruise of the R/V *Professor Vodyanitsky* which took place in June 30 – July 18, 2016 in the central sector of the northern Black Sea were used (31°–36.5°E, 43°–45°N) [10]. CTD measurements were performed using the SBE 911plus CTD probe. The total number of stations amounted to 106. At 20 stations, the measurements were carried out to depths exceeding 1900 m; their location is schematically shown in Fig. 1. The paper analyzes the profiles of potential temperature (θ), salinity (S) and potential density (σ_θ) obtained with meter resolution at these stations. Firstly, the initial profiles were subjected to low-frequency depth filtering to suppress the high-frequency component of the measurement noise. For this purpose, a triangular window-type filter with a base (L_{Filtr}) of 17 m was used.

Fig. 2 shows the potential temperature and salinity profiles in the sea layer deeper than 1500 m obtained at all stations (thin gray lines). The red (station 73) and blue (station 88) lines indicate the profiles with the maximum deviation from the average profile shown in the figure by the thick black line. The range of potential temperature changes within the BCL for the entire ensemble of stations was $1.6 \cdot 10^{-3}$ °C, salinity – $1.2 \cdot 10^{-3}$ psu, which is in good agreement with the previously published data [1, 2, 4].

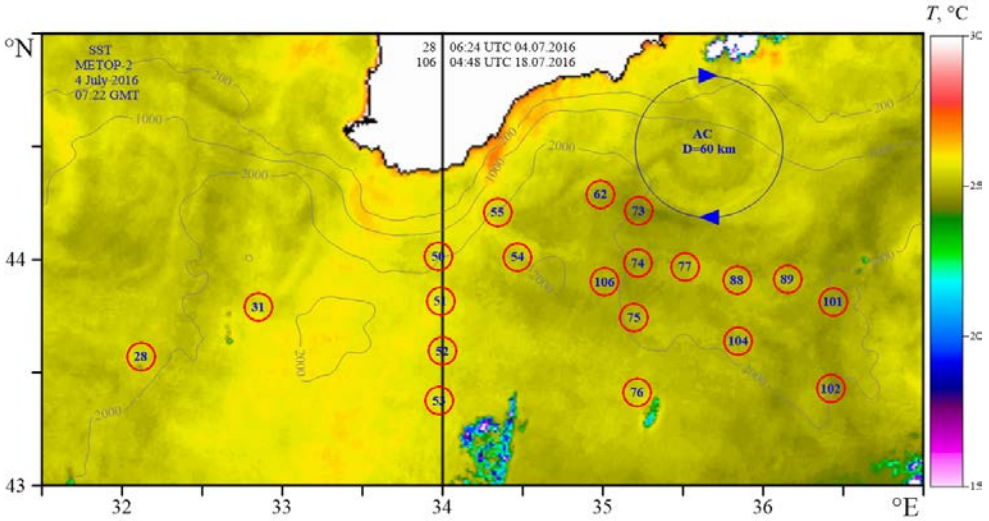

F i g. 1. Location of the stations where sounding depth exceeded 1900 m on the map of bathymetry (ETOPO1) and sea surface temperature (MetOp-2 from 04.07.2016). Blue circle marks the anticyclonic eddy. Stations numbering is in a chronological order and corresponds to the records in the ship's logbook

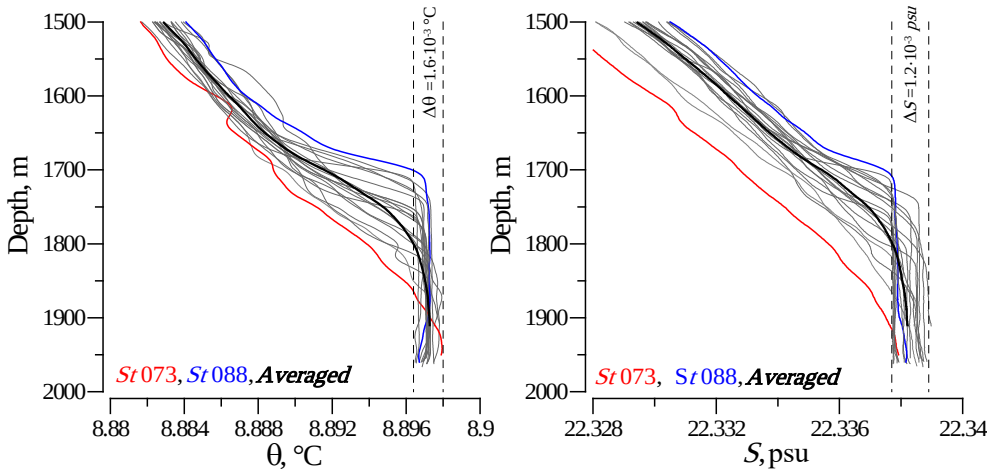

F i g. 2. Potential temperature (*left*) and salinity (*right*) profiles for all the stations (red line denotes the profile for station 73, blue line – for station 88 and black one – average profile)

Let us note that the variability ranges of hydrological parameters in the BCL from station to station slightly exceed the accuracy of the sensors declared by the CTD probe manufacturer. For example, the initial accuracy of a temperature sensor is $1 \cdot 10^{-3}$ °C. It should also be noted that without additional metrological certification of probe sensors, as was done in [1], the absolute values of the measured parameters will have an uncertain component caused by the change in calibration coefficients over time. This is well illustrated by the data presented in [2]. In accordance with the technical documentation, the time drift of the temperature sensor is $2 \cdot 10^{-4}$ °C per month, which allows to hope that, over an

observation interval of about two weeks, the temporal drift of the sensors will not significantly affect the quality of the analysed data and the correctness of the conclusions drawn.

Results and discussion

In the study, the BCL upper boundary was determined by the value of the squared buoyancy frequency ($N^2(z) = \frac{g}{1000 + \sigma_\theta} \frac{\partial \sigma_\theta}{\partial z}$, where $g = 9.81$ m/s^2 is the free fall acceleration; σ_θ is the potential density), equal to $5 \cdot 10^{-8}$ (rad/s)^2, which was convenient for the set of stations under consideration (indicated by the black arrow in Fig. 3).

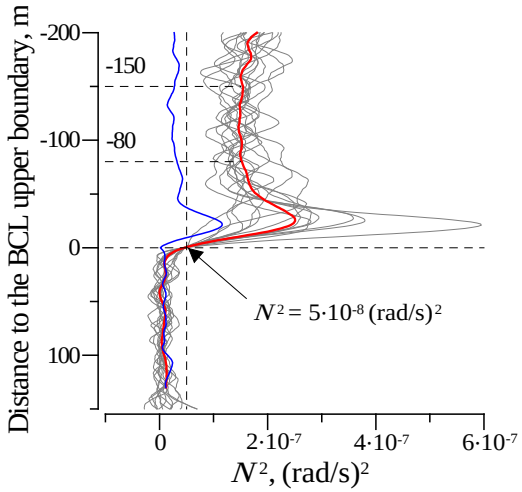

F i g. 3. Dependence of the squared buoyancy frequency upon the distance to the BCL upper boundary. Gray lines are the profiles based on the measurement data, red line is the average profile and blue one is standard deviation from the average profile

Based on the average profiles in Fig. 3, the vertical turbulent diffusion coefficient (K_{G03}) was estimated in the layer 80–150 m above the BCL upper boundary (marked with dashed lines) to subsequently determine the heat and salt fluxes from the deep sea layers. For this, parametrization [11] was used, which relates the desired parameter with field data collected with a small-scale resolution in regions remote from the places of internal wave generation. The parametrization takes into account the geographic location of the measurement area and the deviation of the internal wave spectrum from the canonical form GM76 [12]. The applied formula [13] was used for the calculation

$$K_{G03} = K_0 \frac{\left\langle \xi_z^2 \right\rangle^2}{\left\langle \xi_z^2 \right\rangle_{GM}^2} h_2(R_\omega)\, j(f/N),$$

$$j(f/N) = \frac{f \operatorname{arccos} h(N/f)}{f_{30} \operatorname{arccos} h(N_0/f_{30})},$$

$$h_2(R_\omega) = \frac{1}{6\sqrt{2}} \frac{R_\omega (R_\omega + 1)}{\sqrt{R_\omega - 1}},$$

where $K_0 = 5 \cdot 10^{-6}$ m^2/s; ξ_Z is the strain; f is the local inertial frequency at 44°N (Fig. 1); f_{30} is the inertial frequency at 30°N, $N_0 = 5.24 \cdot 10^{-3}$ rad/s, $\langle\ \rangle$ is operator of averaging values over the entire ensemble of stations. Supposing that $\langle N^2 \rangle = 1.5 \cdot 10^{-7}$ (rad/s)^2, we obtain $j(f/N) = 0.57$. The kinetic and potential energy (R_ω) ratio in the internal wave for the Black Sea is about 12 [14, 15], which implies that $h_2(R_\omega) = 5.56$. The average measured value of the squared deformation over the entire ensemble of stations was

$$\langle \xi_z^2 \rangle = \langle (N^2 - \langle N^2 \rangle) \rangle / \langle N^2 \rangle^2 = 2.8 \cdot 10^{-2}.$$

The average value of the squared deformation for the canonical spectrum of internal waves GM76 [16, 17] was calculated from the following relation

$$\langle \xi_z^2 \rangle_{\mathrm{GM}\,76} = \int_0^1 F_{\mathrm{GM}\,76}(k) \cdot H_{\mathrm{Filtr}}(k) \cdot H_{Dif}(k) \cdot dk = 3.4 \cdot 10^{-2},$$

where $F_{\mathrm{GM}\,76}(k)$ is the spectral deformation density as given in [18]; $H_{\mathrm{Filtr}}(k) = \left(\frac{\mathrm{Sin}(\pi \cdot L_{\mathrm{Filtr}} \cdot k)}{\pi \cdot L_{\mathrm{Filtr}} \cdot k} \right)^4$ is the transfer function of preliminary low frequency filtering, $H_{Dif}(k) = \left(\frac{\mathrm{Sin}(\pi \cdot 2 \cdot k)}{\pi \cdot 2 \cdot k} \right)^2$ is the transfer function of differentiation at a depth increment of 2 m; k is the vertical wave number. As a result, we obtain the value $K_{\mathrm{G}03} = 1.1 \cdot 10^{-5}$ m^2/s, close to the background value of the coefficient (10^{-5} m^2/s) in *PP*81 parametrization [19], applied in the numerical simulation. We shall note that the obtained value of the coefficient of vertical turbulent diffusion significantly exceeds the values of the coefficients of molecular heat ($k_T = 1.4 \cdot 10^{-7}$ м^2/с) and salt ($k_S = 1.1 \cdot 10^{-9}$ м^2/с) diffusion.

Fig. 4 shows the average profiles of potential temperature, salinity and their vertical derivatives (θ_Z and S_Z, respectively) depending on the distance to the BCL upper boundary. In [4], an increase in the values of vertical gradients of hydrological parameters directly above the BCL in a transition layer 25–50 m thick is observed. In our case, an increase in the vertical gradients of temperature and salinity begins to be traced at a distance of 150 m above the BCL upper boundary. At this depth, there is no influence of dynamic processes on stable density stratification and no internal waves are generated. The maximum vertical gradients of temperature and salinity are observed 25 m above the BCL upper boundary.

The temperature derivative value at the maximum is three times greater than its value, which was established at 150 m above the upper boundary of the BCL, while for salinity, similar parameters differ only by a factor of two.

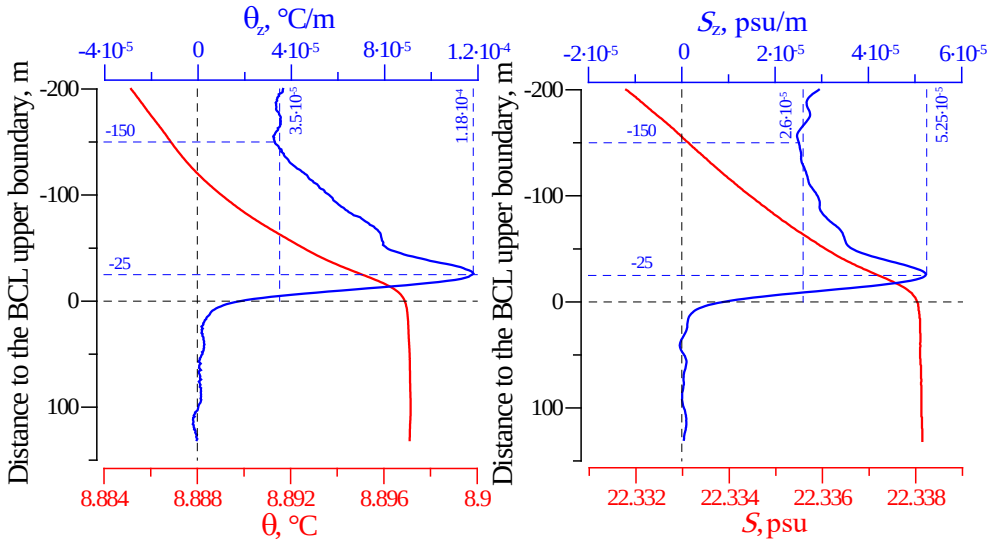

F i g. 4. Average vertical distribution of potential temperature (*left*) and salinity (*right*) in the vicinity of the BCL upper boundary. Red lines are the mean values and blue lines are the vertical derivatives

Vertical heat flux (F_{Heat}) at 150 m over the BCL upper boundary was calculated according to the following relation

$$F_{\text{Heat}} = \rho_{\dot{W}} C_{\cdot W} \; K_{\text{G03}} \cdot \theta_z = \; 1.6 \text{ mW/m}^2,$$

where ρ_W is the water density (1017 kg/m^3); C_W is the heat capacity of water (4.2·10^3 J/(°C·kg)); θ_Z is the vertical derivative of potential temperature (3.5·10^{-5} °C/m). The obtained value is less than 1/20 of the mean value of the geothermal heat flux, which is usually assumed to be 40 mW/m^2 [5, 20]. This means that almost entire geothermal heat flux is dissipated in the BCL, providing slow convective mixing that maintains a uniform vertical distribution of hydrological, hydrochemical and hydrooptical parameters.

The vertical salt flux on the same horizon was determined by the following relation

$$F_{\text{Salt}} = \rho_{\dot{W}} \; K_{\text{G03}} \cdot S_z = 2.9 \cdot 10^{-7} \text{ g/(m}^2\text{·s)},$$

where S_z is the vertical derivative of salinity (2.6·10^{-5} psu/m). In accordance with this fact, the salinity decrease in the homogeneous bottom 300 m layer will occur at a rate of about 3·10^{-5} psu/year and will reach a value of 10^{-3} psu within 33 years. The upward salt flux existence implies the presence of a mechanism for its replenishment in the lower sea layers to maintain the salt balance [21]. There are no field data in the literature that indicate a constant supply of salt to the bottom layer. However, there is an assumption that salt intrusions into the lower sea layers

occur episodically [22]. It is confirmed by the “salinity wave” discovery in 2005–2009 [5], showing a time-limited anomalous increase in salinity at depths over 1400 m.

The BCL upper boundary depth (Fig. 5) varies from station to station in the range from 1713 to 1922 m. The results obtained confirm the conclusions of [5] that the boundary of the bottom convective layer is not horizontal.

The average depth of the BCL upper boundary was 1800 ± 60 m, which is in good agreement with the data of [1]. A tendency for the BCL upper boundary to rise by 150–200 m during the transition from the western gyre (stations 28, 31) to the eastern one (stations 74–106) can be observed. The rise of isotherms to the east (35°–39°E) at the BCL upper boundary was also noted in the data obtained in June 2002 [4]. It is possible that such a change in the BCL upper boundary depth with increasing longitude is seasonal. In the central part of the polygon (stations 50–55), there is a significant variability in the layer boundary depth with a span over 130 m. Unfortunately, the available data do not allow to determine the characteristic spatiotemporal scales of the observed variability.

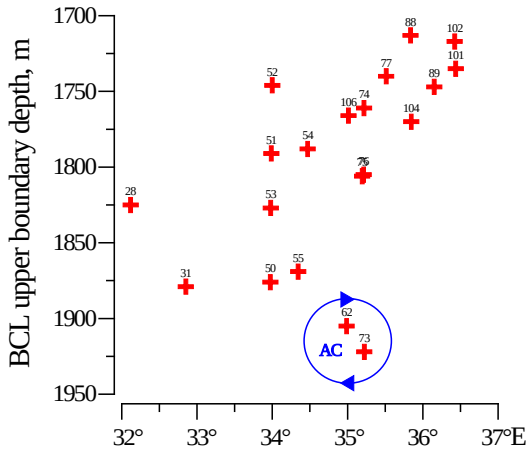

F i g. 5. Position of the BCL upper boundary for all the stations depending on a longitude

Two stations (62 and 73) are of particular interest in the northeastern part of the polygon, where the BCL upper boundary is found at depths over 1900 m. Such BCL boundary position can be explained by the influence of an anticyclonic eddy. Remote sensing data on the sea surface temperature for July 4, 2016 show the existence of an anticyclonic eddy with a characteristic diameter of ~ 60 km (see Fig. 1). Measurements at stations 62 and 73 were carried out on July 11 and 12, 2016, respectively. According to remote sensing data, as of July 12, 2016, there were no signs of eddy structures on the sea surface temperature maps. Presumably, from July 4 to July 12, the eddy shifted to the west and dissipated, but its residual effect is still traced in the deep sea layers and is expressed in the relative depth of isotherms and isohalines (Fig. 2).

The BCL upper boundary position at a depth over 1900 m is extremely rare in observations, for example, such situations were documented in [5] on January 28,

2014 and on March 19, 2014. The sea surface temperature map dated March 22, 2014, according to remote sensing data, shows the presence of a cascade of anticyclonic eddies in the central sector of the southern Black Sea (Fig. 6). This confirms the assumption that anticyclonic eddies can cause anomalous deepening of the BCL upper boundary. Additionally, in favor of the penetration possibility of eddies into the deep layers of the Black Sea, modern data on currents presented in [8] testify that the level of spectral energy of current velocity pulsations near 10^{-6} Hz frequency varies insignificantly between 100 and 1700 m horizons. This may serve as evidence of the presence of mesoscale barotropic dynamic formations passing over the station setting point for 10–11 days [8]. In [23], based on satellite altimetry data, it was shown that the station location area is characterized by the passage of anticyclonic eddies with a radius of 25 km and a movement speed of ~5 cm/s to the southwest along the continental slope, which corresponds to a current velocity variability frequency of 10^{-6} Hz.

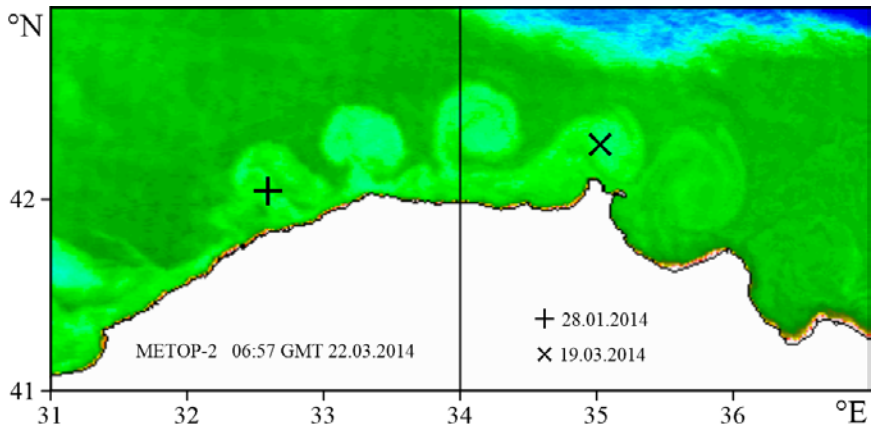

F i g. 6. Sea surface temperature (MetOp-2 from 22.03.2014) and position of the stations where an anomalous deepening of the BCL upper boundary was detected

When considering the variability of the BCL thermohaline characteristics depending on the geographic location of the stations, the following data was obtained. Potential temperature and salinity, on average, show a decrease with increasing longitude (Fig. 7). The temperature and salinity in the BCL are defined as their mean values in the layer from its upper boundary to the sounding depth. For temperature, the value of the squared coefficient of linear correlation (R^2) was 0.25, which does not allow to speak about the significance of its linear relationship with longitude. At the same time, a closer dependence of salinity on longitude is observed (R^2 = 0.75). It was found in [1] that the distribution of hydrological parameters in BCL does not have horizontal gradients. Later, in [24], it was suggested that the BCL waters in the western sea part are warmer and more saline than in the eastern part. The data discussed in this paper support this assumption, especially with regard to salinity. A less close relationship between temperature and longitude can be explained by the spatial heterogeneity of the power of geothermal heat fluxes [20].

For the potential temperature, a dependence with a high value of the squared linear correlation coefficient (R^2 = 0.74) on the BCL thickness was established (Fig. 8). Higher temperatures are noted in the western gyre (stations 28, 31), in the anticyclonic eddy (stations 62, 73) and near the continental slope (station 55), where the layer thickness is less than 200 m. A possible reason for the BCL temperature decrease with the layer thickness increase may be the faster heating of thinner layers. The paucity of data does not allow the unambiguous determination whether the observed dependence is a regularity or whether it is typical only for the data obtained at specific stations.

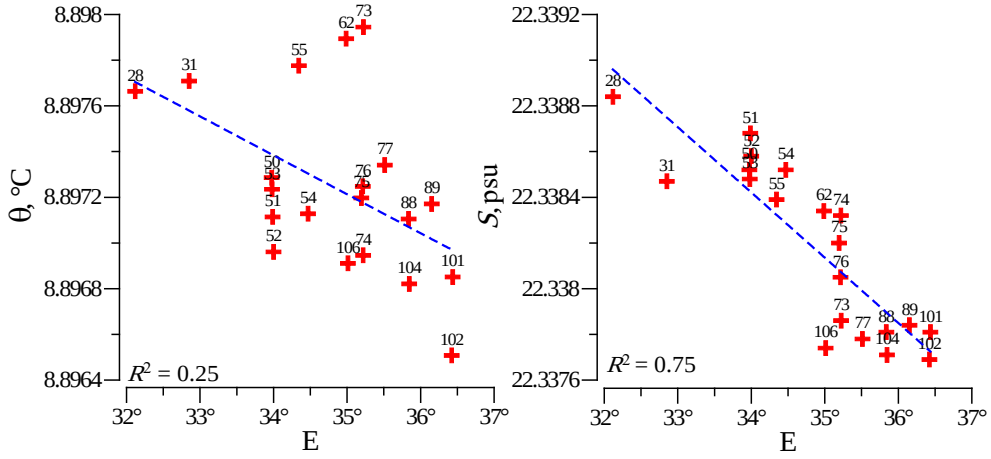

F i g. 7. Dependence of potential temperature and salinity in BCL upon longitude

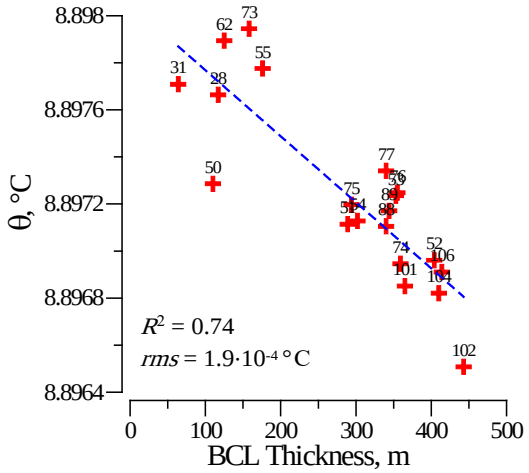

F i g. 8. Dependence of the BCL potential temperature upon its thickness

Conclusion

According to measurements carried out in the summer of 2016 in the northern Black Sea, it is shown that the BCL upper boundary depth varies from station to station in the range of 1713–1922 m. The average depth of the upper boundary of

the layer was 1800 ± 60 m, which is in good agreement with previously published data. A tendency for the upper boundary to rise by 150–200 m during the transition from the western to the eastern gyre was noted.

At two stations, the bottom convective layer is not detected down to depths exceeding 1900 m. This situation is presumably due to the influence of the anticyclonic eddy identified in the measurement area on the sea surface temperature map. The data obtained indicate that eddy movements penetrate into the deep layers of the sea and manifest in a significant deepening of the BCL upper boundary.

The range of variations in potential BCL temperature from station to station was $1.6 \cdot 10^{-3}$ °C, salinity – $1.2 \cdot 10^{-3}$ psu. The variability of BCL thermohaline characteristics depending on the geographic location of the stations shows a decrease in temperature and salinity with increasing longitude. This confirms the assumption made in the works of other authors that the bottom convective layer waters in the western Black Sea are warmer and more saline than in its eastern part.

The BCL potential temperature shows a linear decrease with increasing layer thickness (linear correlation coefficient is 0.74). The highest temperatures are observed in the western gyre, in the anticyclonic eddy and near the continental slope, where the layer thickness is less than 200 m.

Based on the obtained data, estimates of heat and salt fluxes from the deep layers of the sea were carried out. The coefficient of vertical turbulent diffusion at 150 m above the BCL upper boundary was calculated using the G03 parameterization and amounted to $K_{G03} = 1.1 \cdot 10^{-5}$ m^2/s. The corresponding estimated value of the vertical heat flux at 150 m above the BCL upper boundary is $F_{Heat} = 1.6$ mW/m^2, which is less than 1/20 of the mean geothermal heat flux. The calculated value of the vertical salt flux at 150 m above the BCL upper boundary was $F_{Salt} = 2.9 \cdot 10^{-7}$ g/(m^2·s). This means that the decrease in salinity in the homogeneous bottom 300-m layer will occur at a rate of about $3 \cdot 10^{-5}$ psu/year and will reach its spatial variability level in 40 years.

The presented results may be of interest from the viewpoint their reproduction in numerical simulation experiments and further study of the characteristics and dynamics of the Black Sea deep layers.

REFERFENCES

1. Murray, J.W., Top, Z. and Özsoy, E., 1991. Hydrographic Properties and Ventilation of the Black Sea. *Deep Sea Research Part A. Oceanographic Research Papers*, 38(suppl. 2), pp. S663-S689. https://doi.org/10.1016/S0198-0149(10)80003-2
2. Ivanov, V.A. and Belokopytov, V.N., 2013. *Oceanography of the Black Sea*. Sevastopol: ECOSI-Gidrofizika, 210 p.
3. Özsoy, E., Top, Z., White G.N. and Murray, J., 1991. Double Diffusive Intrusions, Mixing and Deep Sea Convection Processes in the Black Sea. In: E. Izdar and J. W. Murray, eds., 1991. *Black Sea Oceanography*. NATO ASI Series, vol. 351. Dordrecht: Springer, pp. 17-42. https://doi.org/10.1007/978-94-011-2608-3_2
4. Falina, A.S. and Volkov, I.I., 2003. On the Fine Structure and Thermohalinic Stability of the Abyssal Water in the Black Sea. *Oceanology*, 43(4), pp. 485-492.

5. Stanev, E.V., Chtirkova, B. and Peneva, E., 2021. Geothermal Convection and Double Diffusion Based on Profiling Floats in the Black Sea. *Geophysical Research Letters*, 48(2), e2020GL091788. https://doi.org/10.1029/2020GL091788

6. Volkov, I.I., Rimskaya-Korsakova, M.N. and Grinenko, V.A., 2007. Chemical and Isotopic Uniformity of the Bottom Convective Water Layer in the Black Sea. *Doklady Earth Sciences*, 414(1), pp. 625-629. https://doi.org/10.1134/S1028334X07040290

7. Man'kovskii, V.I., 2003. Specific Features of the Vertical Distribution of the Beam Attenuation Coefficient in the Short- and Long-Wave Spectral Bands in Deep-Water Layers of the Hydrogen-Sulfide Zone and in the Bottom Layer of the Black Sea. *Physical Oceanography*, 13(3), pp. 183-187. doi:10.1023/A:1025099003581

8. Klyuvitkin, A.A., Ostrovskii, A.G., Lisitzin, A.P. and Konovalov, S.K., 2019. The Energy Spectrum of the Current Velocity in the Deep Part of the Black Sea. *Doklady Earth Sciences*, 488(2), pp. 1222-1226. doi:10.1134/S1028334X1910012X

9. Morozov, A.N. and Mankovskaya, E.V., 2020. Cold Intermediate Layer of the Black Sea according to the Data of the Expedition Field Research in 2016–2019. *Ecological Safety of Coastal and Shelf Zones of Sea*, (2), pp. 5-16. doi:10.22449/2413-5577-2020-2-5-16 (in Russian).

10. Morozov, A.N. and Mankovskaya, E.V., 2019. Seasonal Variability of Currents Structure in the Black Sea Northern Part from Field Measurements in 2016. *Fundamentalnaya i Prikladnaya Gidrofizika*, 12(1), pp. 15-20. doi:10.7868/S2073667319010027 (in Russian).

11. Gregg, M.C., Sanford, T.B. and Winkel, D.P., 2003. Reduced Mixing from the Breaking of Internal Waves in Equatorial Waters. *Nature*, 422, pp. 513-515. https://doi.org/10.1038/nature01507

12. Polzin, K.L., Toole, J.M. and Schmitt, R.W., 1995. Finescale Parameterizations of Turbulent Dissipation. *Journal of Physical Oceanography*, 25(3), pp. 306-328. https://doi.org/10.1175/1520-0485(1995)025<0306:FPOTD>2.0.CO;2

13. Kunze, E., Firing, E., Hummon, J.M., Chereskin, T.K. and Thurnherr, A.M., 2006. Global Abyssal Mixing Inferred from Lowered ADCP Shear and CTD Strain Profiles. *Journal of Physical Oceanography*, 36(8), pp. 1553-1576. https://doi.org/10.1175/JPO2926.1

14. Morozov, A.N. and Lemeshko, E.M., 2014. Estimation of Vertical Turbulent Diffusion Coefficient by CTD/LADCP-Measurements in the Northwestern Part of the Black Sea in May, 2004. *Morskoy Gidrofizicheckiy Zhurnal*, (1), pp. 58-67 (in Russian).

15. Morozov, A.N., Mankovskaya, E.V. and Fedorov, S.V., 2021. Inertial Oscillations in the Northern Part of the Black Sea Based on the Field Observations. *Fundamentalnaya i Prikladnaya Gidrofizika*, 14(1), pp. 43-53. doi:10.7868/S2073667321010044 (in Russian).

16. Garrett, C. and Munk, W., 1975. Space-Time Scales of Internal Waves: A Progress Report. *Journal of Geophysical Research*, 80(3), pp. 291-297. https://doi.org/10.1029/JC080i003p00291

17. Cairns, J.L. and Williams, G.O., 1976. Internal Wave Observations from a Midwater Float, 2. *Journal of Geophysical Research*, 81(12), pp. 1943-1950. https://doi.org/10.1029/JC081i012p01943

18. Fer, I., 2006. Scaling Turbulent Dissipation in an Arctic Fjord. *Deep Sea Research Part II: Topical Studies in Oceanography*, 53(1–2), pp. 77-95. https://doi.org/10.1016/j.dsr2.2006.01.003

19. Pacanowski, R.C. and Philander, S.G.H., 1981. Parameterization of Vertical Mixing in Numerical Models of Tropical Oceans. *Journal of Physical Oceanography*, 11(11), pp. 1443-1451. https://doi.org/10.1175/1520-0485(1981)011<1443:POVMIN>2.0.CO;2

20. Kutas, R.I., 2010. Geothermal Conditions of the Black Sea Basin and Its Surroundings. *Geofizicheskiy Zhurnal*, 32(6), pp. 135-158. https://doi.org/10.24028/gzh.0203-3100.v32i6.2010.117453 (in Russian).

21. Eremeev, V.N., Ivanov, L.I., Samodurov, A.S. and Duman, M., 1998. The Near-Bottom Boundary Layer in the Black Sea: Hydrological Structure and Modelling. *Physical Oceanography*, 9(2), pp. 79-101. https://doi.org/10.1007/BF02525515

22. Stewart, K., Kassakian, S., Krynytzky, M., DiJulio and D., Murray, J.W., 2005. Oxic, Suboxic, and Anoxic Conditions in the Black Sea. In: A. Gilbert, V. Yanko-Hombach and N. Panin, eds., 2005. *Climate Change and Coastline Migration as Factors in Human Adaptation to Circum-Pontic Region: From Past to Forecast*. New York, NY: Kluwer, pp. 437-452.

23. Kubryakov, A.A. and Stanichny, S.V., 2015. Mesoscale Eddies in the Black Sea from Satellite Altimetry Data. *Oceanology*, 55(1), pp. 56-67. https://doi.org/10.1134/S0001437015010105

24. Falina, A.S. and Volkov, I.I., 2005. The Influence of Double Diffusion on the General Hydrological Structure of the Deep Waters in the Black Sea. *Oceanology*, 45(1), pp. 16-25.

About the authors:

Alexey N. Morozov, Senior Research Associate, Marine Hydrophysical Institute of RAS (2 Kapitanskaya Str., Sevastopol, Russian Federation, 299011), Ph.D. (Tech. Sci.), **ORCID ID: 0000-0001-9022-3379**, **Scopus Author ID: 7202104940, ResearcherID: ABB-4365-2020,** anmorozov@mhi-ras.ru

Ekaterina V. Mankovskaya, Senior Research Associate, Marine Hydrophysical Institute of RAS (2 Kapitanskaya Str., Sevastopol, Russian Federation, 299011), Ph.D. (Tech. Sci.), **ORCID ID: 0000-0002-4086-1687**, **Scopus Author ID: 57192647961, ResearcherID: AAB-5303-2019**, emankovskaya@mhi-ras.ru

Contribution of the co-authors:

Alexey N. Morozov – statement of the problem, processing of measurement data, analysis of research results, preparation of graphic materials, editing and supplementing of the paper text

Ekaterina V. Mankovskaya – processing of measurement data, collection of information for research, discussion of the research results, formulation of conclusions, preparation of the paper text

The authors have read and approved the final manuscript.
The authors declare that they have no conflict of interest.